THE JOURNAL OF BIOLOGICAL CHEMISTRY
Vol. 279, No. 29, Issue of July 16, pp. 30588–30599, 2004
Printed in U.S.A.

Mechanical Strain on Osteoblasts Activates Autophosphorylation of Focal Adhesion Kinase and Proline-rich Tyrosine Kinase 2 Tyrosine Sites Involved in ERK Activation*

Received for publication, December 4, 2003, and in revised form, March 1, 2004
Published, JBC Papers in Press, April 19, 2004, DOI 10.1074/jbc.M313244200

Nadia Boutahar, Alain Guignandon, Laurence Vico, and Marie-Hélène Lafage-Proust‡

From the Laboratoire de Biologie du Tissu Osseux, INSERM, E366, 15 Rue Ambroise Paré, 42023 Saint-Etienne Cedex 02, France

The mechanisms involved in the mechanical loading-induced increase in bone formation remain unclear. In this study, we showed that cyclic strain (CS) (10 min, 1% stretch at 0.25 Hz) stimulated the proliferation of overnight serum-starved ROS 17/2.8 osteoblast-like cells plated on type I collagen-coated silicone membranes. This increase was blocked by MEK inhibitor PD-98059. Signaling events were then assessed 0 min, 30 min, and 4 h after one CS period with Western blotting and co-immunoprecipitation. CS rapidly and time-dependently promoted phosphorylation of both ERK2 at Tyr-187 and focal adhesion kinase (FAK) at Tyr-397 and Tyr-925, leading to the activation of the Ras/Raf/MEK pathway. Cell transfection with FAK mutated at Tyr-397 completely blocked ERK2 Tyr-187 phosphorylation. Quantitative immunofluorescence analysis of phosphotyrosine residues showed an increase in focal adhesion plaque number and size in strained cells. CS also induced both Src-Tyr-418 phosphorylation and Src to FAK association. Treatment with the selective Src family kinase inhibitor pyrazolopyrimidine 2 did not prevent CS-induced FAK-Tyr-397 phosphorylation suggesting a Src-independent activation of FAK. CS also activated proline-rich tyrosine kinase 2 (PYK2), a tyrosine kinase highly homologous to FAK, at the 402 phosphorylation site and promoted its association to FAK in a time-dependent manner. Mutation of PYK2 at the Tyr-402 site prevented the ERK2 phosphorylation only at 4 h. Intra and extracellular calcium chelators prevented PYK2 activation only at 4 h. In summary, our data showed that osteoblast response to mitogenic CS was mediated by MEK pathway activation. The latter was induced by ERK2 phosphorylation under the control of FAK and PYK2 phosphorylation orchestrated in a time-dependent manner.

It is now well evidenced that mechanical stimulation can increase bone mass *in vivo* (1) through an increase in the number of osteoblasts, the bone-forming cells. *In vitro* experiments have revealed that physical forces act directly at the cellular level and showed that bone cells are able to respond physiologically to mechanical stress (2, 3). It was shown that cyclic mechanical loading is more effective in inducing osteoblast proliferation and gene expression than is static loading (4). There is a large body of evidence showing that extracellular signal-regulated kinase 1/2 (ERK1/2)[1] controls cell proliferation in various cell types, including osteoblasts (5). Recent reports demonstrated that mechanical strain is able to activate ERK1/2 in several adherent cells such as mesangial cells (6), smooth muscle cells (7), and chondrocytes (8). In osteoblasts, ERK activation was mostly reported in fluid flow (9–12), centrifugation (13), or magnetic drag force (14) experiments and in only one study using cyclic stretch (albeit combined with fluid flow) (15). However, cell stretch appears to be a relevant model of mechanical stimulus in the bone field (16, 17) and provides specific osteoblastic responses (18). The molecular mechanisms that control mechanically induced ERK activation in osteoblasts remain obscure. Integrins are strong candidates as mechanotransducers in mechanical strain-induced ERK activation (19, 20). Indeed, integrin-mediated cell attachment activates many intracellular signaling pathways such as tyrosine phosphorylation cascades, calcium influx, inositol lipid turnover, and mitogen-activated protein kinase (MAPK) activation, (21, 22). Thus, the first aim was to determine whether ERK1/2 activation mediated stretch-induced mitogenicity in a cyclic strain model using cell stretch. In particular, we focused on tyrosine-phosphorylated forms of proteins activated by mechanical strain. Focal adhesion kinase (FAK) is a cytoplasmic protein tyrosine kinase that has been reported to play an important role in integrin-mediated signal transduction pathways (22). Indeed, some studies showed that the adhesion of suspended cells onto components of the extracellular matrix induces the activation of proteins such as FAK at multiples sites, including Tyr-397 (23, 24), the only apparent autophosphorylation site (25–27). This autophosphorylation is critical, because it creates a high affinity binding site for the Src homology 2 domain of Src family kinases, leading to a signaling complex between FAK and Src family kinases (24, 28, 29). This association of FAK-Src, together with the Grb2 adaptor protein, represents one mechanism of activation of ERK by FAK (30). This cascade of phosphorylation events and protein-protein interaction was reported upon integrin binding. However, it is not known whether similar events are induced by the mechanical strain applied to adherent cells.

Among strain-induced tyrosine phosphorylated proteins we found expression of the related adhesion focal tyrosine kinase, also known as proline-rich tyrosine kinase 2 (PYK2) (31), cell adhesion kinase β (32), or calcium-dependent protein-tyrosine

* This work was supported by European Research In Space and Terrestrial Osteoporosis (ERISTO). The costs of publication of this article were defrayed in part by the payment of page charges. This article must therefore be hereby marked "*advertisement*" in accordance with 18 U.S.C. Section 1734 solely to indicate this fact.

‡ To whom correspondence should be addressed. Tel.: 33-477-42-14-54; Fax: 33-477-57-55-72; E-mail: lafagemh@univ-st-etienne.fr.

[1] The abbreviations used are: ERK, extracellular signal-regulated kinase; FAK, focal adhesion kinase; FCS, fetal calf serum; HA, hemagglutinin A; MAPK mitogen-activated protein kinase; PBS, phosphate-buffered saline; PI, proliferation index; PYK2, proline-rich tyrosine kinase 2; BAPTA-AM, 1,2-bis (*o*-aminophenoxy)ethane-*N*,*N*,*N*′,*N*′-tetraacetic acid tetra(acetoxymethyl)ester.

kinase (33) (for convenience, it is referred to here as PYK2). PYK2 (116 kDa) shares a 45% overall sequence similarity with FAK (125 kDa), and four of the six FAK tyrosine phosphorylation sites (Tyr-397, -576, -577, and -925) are conserved at analogous positions in PYK2 (Tyr-402, -579, -580, and -881). Interestingly, PYK2 was found to be activated in osteoblasts by fluoroaluminate, a strong bone anabolic agent (34), suggesting that this tyrosine kinase might play a critical role in the stimulation of osteoblast proliferation (35). It has been shown that the tyrosine phosphorylation of PYK2 was markedly enhanced when the cytoplasmic free Ca^{2+} concentration is increased (31). In our study, we therefore began to analyze the potential involvement of Ca^{2+} regulatory role in PYK2 activation by mechanical strain.

EXPERIMENTAL PROCEDURES

Materials—Y402F-c-Myc-tagged PYK2 and Y397F-HA-tagged FAK were kindly provided by Dr. Shelton Earp (University of North Carolina Chapel Hill, NC). Horseradish peroxidase-conjugated goat anti-rabbit P0448 and horseradish peroxidase-conjugated horse anti-mouse P0447 were obtained from DAKO, and the phosphospecific antibodies anti-ERK-Tyr(P)-187, anti-FAK-Tyr(P)-397, anti-FAK-Tyr(P)-925, anti-Src-Tyr(P)-418, and anti-PYK2-Tyr(P)-402 were purchased from Biosource International (Camarillo, CA). Enhanced chemiluminescence detection reagents were obtained from Pierce. The stripping solution Re-Blot Plus was obtained from Chemicon International (Temecula, CA). ERK2 (D-2), c-Src (B-12), Tyr(P) (PY99), and FAK (H-1) were obtained from Santa Cruz Biotechnology (Santa Cruz, CA). Pyrazolopyrimidine 2 (PP-2) and PD-98059 inhibitor were obtained from Calbiochem. Anti-HA and anti-c-Myc mouse monoclonal antibodies were obtained from Santa Cruz Biotechnology.

Cells—We used ROS 17/2.8 osteoblast-like cells, a well defined cell line (36) with the characteristics of mature osteoblasts (alkaline phosphatase activity, osteocalcin and type I collagen expression, and the ability to mineralize), and the mouse osteoblastic cell line MC3T3-E1, which consists of primary osteoblastic cells from old male Wistar rats. Briefly, after removing soft tissues, metaphyses reduced to ~2-mm-wide fragments were submitted to fractional digestions every 15 min with 1 mg/ml clostridium histolyticum neutral collagenase (Sigma) in medium at 37 °C three times with stirring. Collagenase was neutralized with medium supplemented with 15% fetal calf serum (FCS). Cell suspension was then centrifuged at 1300 rpm for 5 min and resuspended in α-minimum Eagle's medium supplemented with 10% FCS (Sigma), 50 μg/ml ascorbic acid, and 2 mg/ml β-glycerophosphate. The medium was changed after the first 24 h to remove non-adherent cells. Cells were grown in humidified atmosphere of 5% CO_2 at 37 °C. ROS 17/2.8 cells were cultured in Dulbecco's modified Eagle's medium, whereas MC3T3-E1 and primary rodent osteoblastic cells were cultured in α-minimum Eagle's medium supplemented with 10% FCS, 2 mM L-glutamine, 100 units/ml penicillin, and 0.1 mg/ml streptomycin. After reaching a subconfluent state, cells were trypsinized with 1× trypsin-EDTA and plated onto flexible type I collagen-coated, silicon-bottomed, six-well culture plates (Bioflex; Flexcell Corp., McKeesport, PA).

Cyclic Deformation—The Flexcell Strain Unit Fx-3000 (Flexcell Corp.) was used for the application of mechanical stretch to osteoblasts (37). Cells were plated in six-well tissue culture dishes with type I collagen-coated, flexible silicone bottoms (Bioflex; Flexcell Corp.) at $5{\cdot}10^4$ cells per well density for proliferation studies and $1{\cdot}10^5$ cells per well for signal transduction studies. Seventy-two hours after seeding, cells were serum-starved overnight and then subjected to mechanical deformation. Mechanical deformation was induced with a Flexercell strain unit, which consists of a vacuum manifold regulated by solenoid valves that are controlled by a computer timer program. The Bioflex baseplate contain the Bioflex loading station that consists of six buttons per plate that insert into each plate, allowing a uniform magnitude of the strain across 85% of the surface of the flexible well. For these experiments a negative pressure of 80 kilopascals was applied through an air pump to the culture plate, bottoms were deformed to a known percentage of elongation, and then the membranes were released to their original conformation. The experimental regimens used in this study delivered 1% elongation at a rate of 15 cycles/min (a 2-s deformation period followed by a 2-s neutral position). Cells remained adherent, and the deformation of the membrane is directly transmitted to cells. Unstretched cells grown on Bioflex plates were used as controls.

Proliferation Studies—ROS 17/2.8 cell proliferation was analyzed with PKH26 (38, 39) according to the manufacturer's instructions (Sigma). PKH26 is a fluorescent reporter molecule that incorporates into the cell membrane and is equally distributed to daughter cells following division. It was shown that PKH26 labeling is stable and reproducible and has no effect on cell proliferation (40). Cell suspension was washed in PBS/EDTA (5 μM) and incubated in $4{\cdot}10^{-6}$ M PKH26 staining solution for 4 min at room temperature. The reaction was stopped by the addition of 2 ml of FCS and 4 ml of proliferation medium. Cells were centrifuged at 400 × *g* for 10 min and washed with complete medium to remove cells from the staining solution. Then, cells were seeded at $5{\cdot}10^4$ cells onto type I collagen-precoated flexible membranes. An aliquot was fixed at day 0 in 2% paraformaldehyde and kept at 4 °C until analysis as a time 0 reference. For experimental studies, cells were allowed to recover for 72 h after seeding. Cells were then placed in serum-free media overnight and then submitted to static or strained conditions as described in the previous paragraph ("Cyclic Deformation") in the absence or presence of 20 μM PD-98059 added 30 min before the mechanical stimulus (41). When indicated, cells were fixed in 2% paraformaldehyde and kept at 4 °C until analysis. Analysis was performed on a FACStar^{plus} cell sorter with a 585/42-nm bandpass filter using the Cell Quest program. Each analysis was carried out on a minimum of 5×10^4 cells. Deconvolution of the cell fluorescence into peaks was performed using the Cell Proliferation Model program ran on Modftit 2.0 software. Parameters calculated included the percentage of cells in each subsequent generation, the proliferation index (PI), and the goodness of fit measured by a reduced χ^2. The PI, a measure of the proliferation activity of total cell population, was calculated by ModFit 2.0 using Equation 1,

$$\mathrm{PI} = \sum_{K=0}^{K=n} A_k \Big/ \sum_{K=0}^{K=n} \frac{A_k}{2^k} \qquad \text{(Eq. 1)}$$

in which A_k is the summation of the Gaussian areas in each generation and k equals the generation number. PI represents the total expansion of the parent generation as described by $N_k = 2^k{\cdot}N_0$ or $N_k = \mathrm{PI}{\cdot}N_0$, where N_0 is the number of cells in the parent generation. Therefore, $\mathrm{PI} = 2^k$ with $k = t/Tg$, where t is the time point considered and Tg is the generation time. Data are representative of a minimum of two separate experiments performed in triplicate with statistically significant and similar results.

Immunoprecipitation—Cells were lysed in lysis buffer (25 mM Tris, pH 7.5, 150 mM NaCl, 1% Igepal CA-630 (Sigma), 1% sodium deoxycholate, 0.1% SDS, 50 mM sodium fluoride, 10 mM sodium pyrophosphate, 1 mM 4-(2-aminoethyl)benzenesulfonyl fluoride, 0.1 unit/ml aprotinin, 10 μg/ml leupeptin, and 1 mM sodium orthovanadate). Lysates were clarified by centrifugation at 14,000 rpm for 30 min. Supernatants were transferred to fresh tubes. Protein concentration of lysates was determined by using the bicinchoninic acid assay (Pierce).

Immunoprecipitations were typically performed by using 1–2 mg of cell lysate and 2 μg of purified monoclonal or polyclonal antibodies for Tyr(P), FAK, PYK2, Src, and ERK2. After incubation at 4 °C for 2 h on a rotating device, immune complexes were precipitated at 4 °C overnight on a rotating device by using protein A-Sepharose (Sigma). Immunoprecipitates were washed three times with lysis buffer, extracted in 2× SDS-PAGE sample buffer (125 mM Tris-HCl, pH 6.8, 4% SDS, 20% glycerol, 10% β-mercaptoethanol, and 0.025% bromphenol blue) by boiling for 5 min, electrophoresed by SDS-PAGE, and then analyzed by Western blotting.

Western Blot Analysis—After SDS-PAGE, proteins were transferred to nitrocellulose membrane (Bio-Rad). After transfer, membranes were blocked using 5% nonfat dried milk in PBS, pH 7.4, and incubated overnight at 4 °C with the anti-Tyr(P) (PY99), anti-ERK-Tyr(P)-187, anti-FAK-Tyr(P)-397, anti-FAK-Tyr(P)-925, anti-Src-Tyr(P)-418, and anti-PYK2-tyr(P)-402 antibodies. All of these antibodies were used at a concentration of 0.1 μg/ml. Membranes were washed three times with Tris-buffered saline (with 0.1% Tween 20) and then incubated with secondary antibodies (peroxidase-conjugated goat anti-rabbit (1:2000) or peroxidase-conjugated horse anti-mouse (1:6000) for 1 h at room temperature. After washing three times with TBS with 0.1% Tween 20, the immunoreactive bands were visualized using enhanced chemiluminescence detection reagents. Immunoblot were stripped by using mild antibody stripping solution and reprobed with another antibody. Band intensities were determined by densitometry using Scion Image program (Scion Corporation, Frederick, Maryland).

Immunofluorescence Image Analysis—Cells were exposed to mechanical strain, and protein tyrosine phosphorylation was studied by indirect immunofluorescence staining. Cells ($1{\cdot}10^5$ cells per well) were

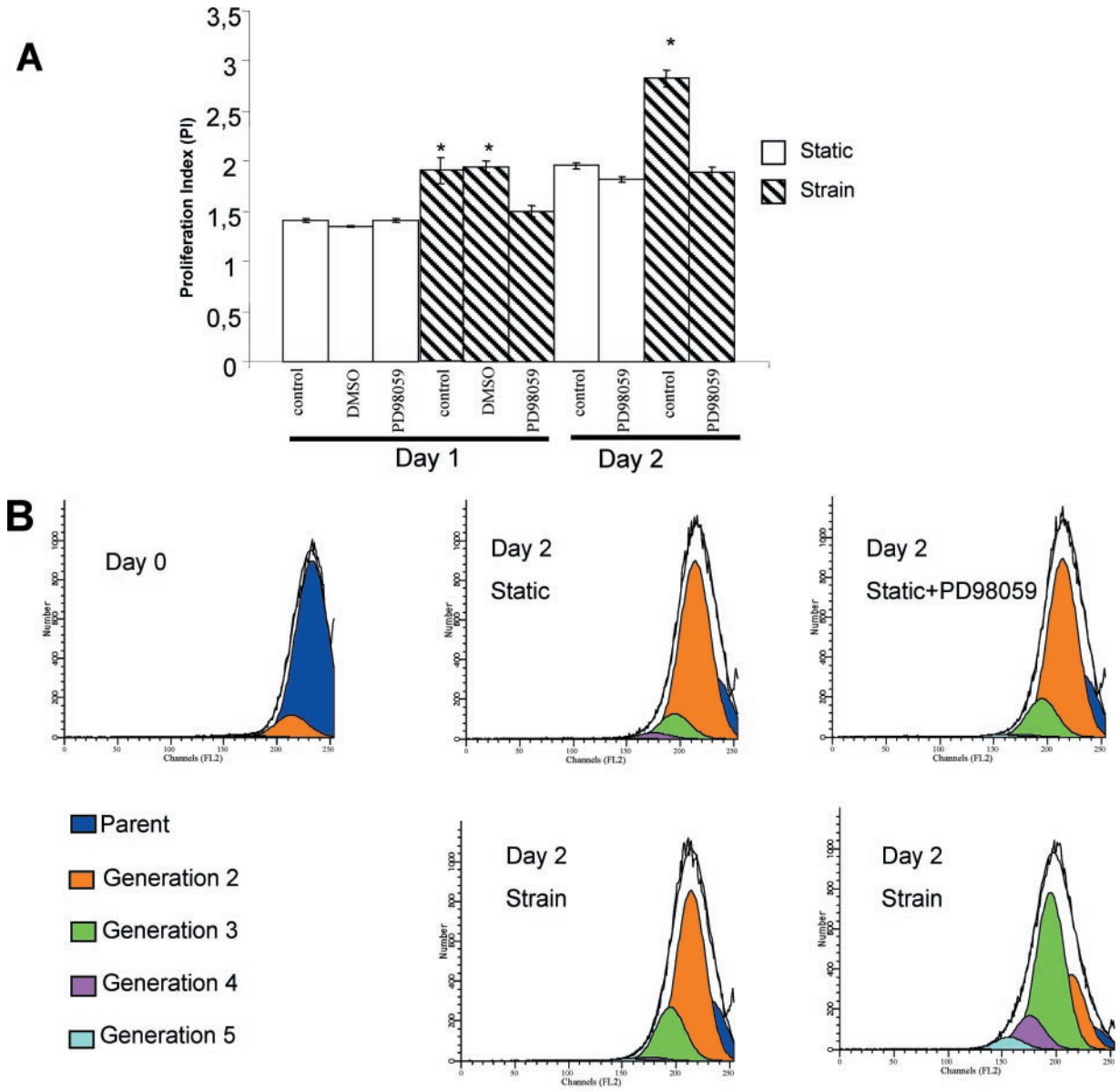

	Day 0	Day 2 static	Day 2 Static + PD98059	Day 2 strain	Day 2 Strain + PD98059
parent (%)	90	21.33	20.62	7.05	19.59
Generation 2 (%)		66.14	63.56	24.93	59.42
Generation 3 (%)		9.32	13.71	52.39	18.79
Generation 4 (%)		2.26	0.92	11.28	1.33
Generation 5 (%)				4.12	
Proliferation index	1	1.75	1.79	2.92	1.84

FIG. 1. **Effect MAPK-ERK kinase (MEK) inhibition on the mitogenic effects of strain.** Cells were labeled with PKH26 membrane labeling and cultured for 72 h in 10% FCS medium. *A*, ROS 17/2.8 cells were serum-starved overnight and then maintained under static (*white bars*) or strained (*hatched bars*) conditions for 24 h (*Day 1*) or 48 h (*Day 2*) before trypsinization and analysis by flow cytometry of PKH26 fluorescence intensity. This analysis was performed in control medium, medium supplemented with Me_2SO vehicle control (*DMSO*), or medium supplemented with the MEK inhibitor PD-98059 (20 μM). The FL2 histograms, *i.e.* PKH-26 profiles, were obtained as described under "Experimental Procedures." The fraction of cells in each generation can be assessed by the PI, a measure of the proliferation activity of the total cell population. A cell sample was used as a reference point (Day 0). *B*, a typical 48-h experiment is shown with the percentage of cell numbers in each generation (table and graphs). All proliferation studies were performed in triplicate, and all data presented here are from one of at least two separate experiments, each of which yielded statistically significant and similar results (*, $p < 0.05$).

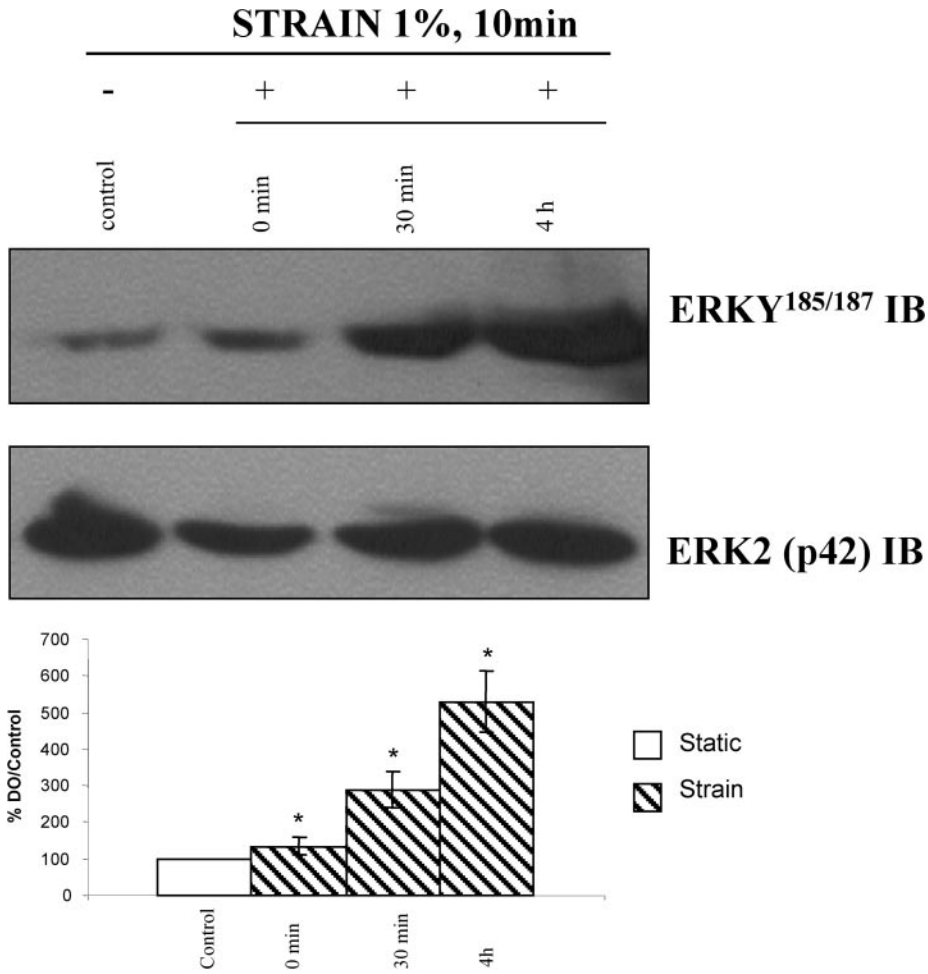

FIG. 2. **Cyclic strain-induced phosphorylation of ERK2 in a time-dependent manner.** ROS 17/2.8 cells plated on flexible bottomed culture plates were subjected to strain for 0 (*control*) or 10 min. Cells were lysed immediately (*0 min*), 30 min, or 4 h after the end of strain. Lysates were immunoblotted with a rabbit polyclonal anti-ERK1/2 MAPK Tyr(P)-185/187 phosphospecific antibody (*ERKY$^{185/187}$ IB*). Equal protein loading was routinely verified by stripping the blot and reblotting with an anti-ERK2 mouse monoclonal antibody (*ERK2 (p42) IB*). Quantification of ERK2-Tyr-187(P) phosphorylation was performed by densitometric scanning of the bands. Values were expressed as mean ± S.E. (*, $p < 0.05$; $n = 3$). *DO*, measurement of optical density of immunoreactive bands on the autoradiogram.

grown for 72 h on flexible type I collagen-coated, silicone-bottomed, six-well culture plates. Cells were then placed in serum-free media overnight and then submitted to static or mechanical strain conditions as described above in the paragraph entitled "Cyclic Deformation." Immunostaining was performed on stretched and control cells at various time points after the end of the stimulation. Cells were fixed in 4% paraformaldehyde for 10 min, washed with cold PBS, and permeabilized with 0.1% Triton X-100 in PBS for 2 min. Mouse monoclonal anti-phosphotyrosine (PY99; 1:100 in 1% PBS/bovine serum albumin) and rabbit polyclonal anti-FAK-Tyr(P)-397 (1:100 in 1% PBS/bovine serum albumin) antibodies were applied for 1 h at 37 °C, and the cells were rewashed in PBS on a rocking platform. Cells were incubated with fluorescein isothiocyanate-conjugated goat anti-mouse or anti-rabbit IgG (1:100 in PBS/bovine serum albumin 1%) for 1h at 37 °C Phosphorylation of tyrosine residues were observed with fluorescence microscope (Leica DMRB, Lyon, France) and acquired with a coded CCD camera (CoolSNAP.fx, Roper Scientific, Evry, France) and Metaview system software (Universal Imaging Corp., Downingtown, PA).

Image Analysis—Cells were analyzed with a semi-automatic image analyzer (Samba-Alcatel, France) on ~120 cells per condition. Quantification was performed on confocal scanning laser images of phosphotyrosine staining (details are reported in Ref. 42). Several morphological features were calculated by the image analysis program. They included the mean area or number of phosphotyrosine-positive spots (42).

Plasmid DNA and Purification—pcDNA3.1/lacZ control vector (Invitrogen), mutated PYK2 cDNAs, pcDNA3-PYK2Y402F, and the mutated FAK cDNA pcDNA3-FAKY397F vector were amplified in ultraMAX^{TM}DH5a-FT^{TM} competent cells (Invitrogen), purified on Qiagen (Courtaboeuf, France) columns, and then resuspended in sterile endotoxin-free saline solution (Qiagen; EndoFree plasmid mega kit). Plasmid DNA concentration was spectrophotometrically measured at 260/280 nm. Plasmids were digested by the specific restriction endonucleases EcoRI and PvuI (Invitrogen), and the quality of non-digested and digested DNA was assessed by 1% agarose gel electrophoresis. At least 90% of non-digested plasmid DNA was supercoiled. Plasmid was stocked at −20 °C before use.

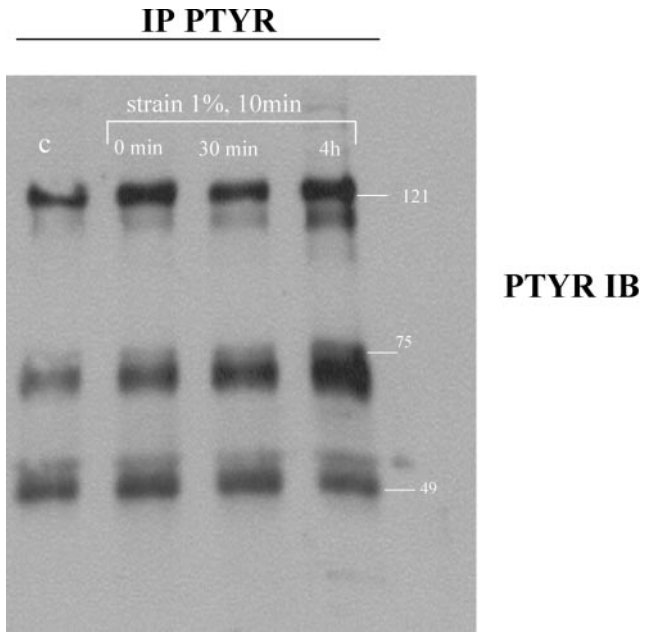

FIG. 3. **Tyrosine phosphorylation induced by cyclic strain.** ROS 17/2.8 cells plated on flexible bottomed culture plates were subjected to strain for 0 (*C*) or 10 min. Cells were lysed immediately (*0 min*), 30 min, or 4 h after the end of strain. Lysates were immunoprecipitated with an anti-phosphotyrosine rabbit polyclonal antibody (*IP PTYR*). Immunoprecipitates were analyzed by SDS-PAGE followed by the transfer of proteins and immunoblotting with a Tyr(P) (PY99) mouse monoclonal antibody (*PTYR IB*). Four predominant bands were seen at 125, 116, 68, and 60 kDa, showing a significant increase in phosphotyrosine after strain.

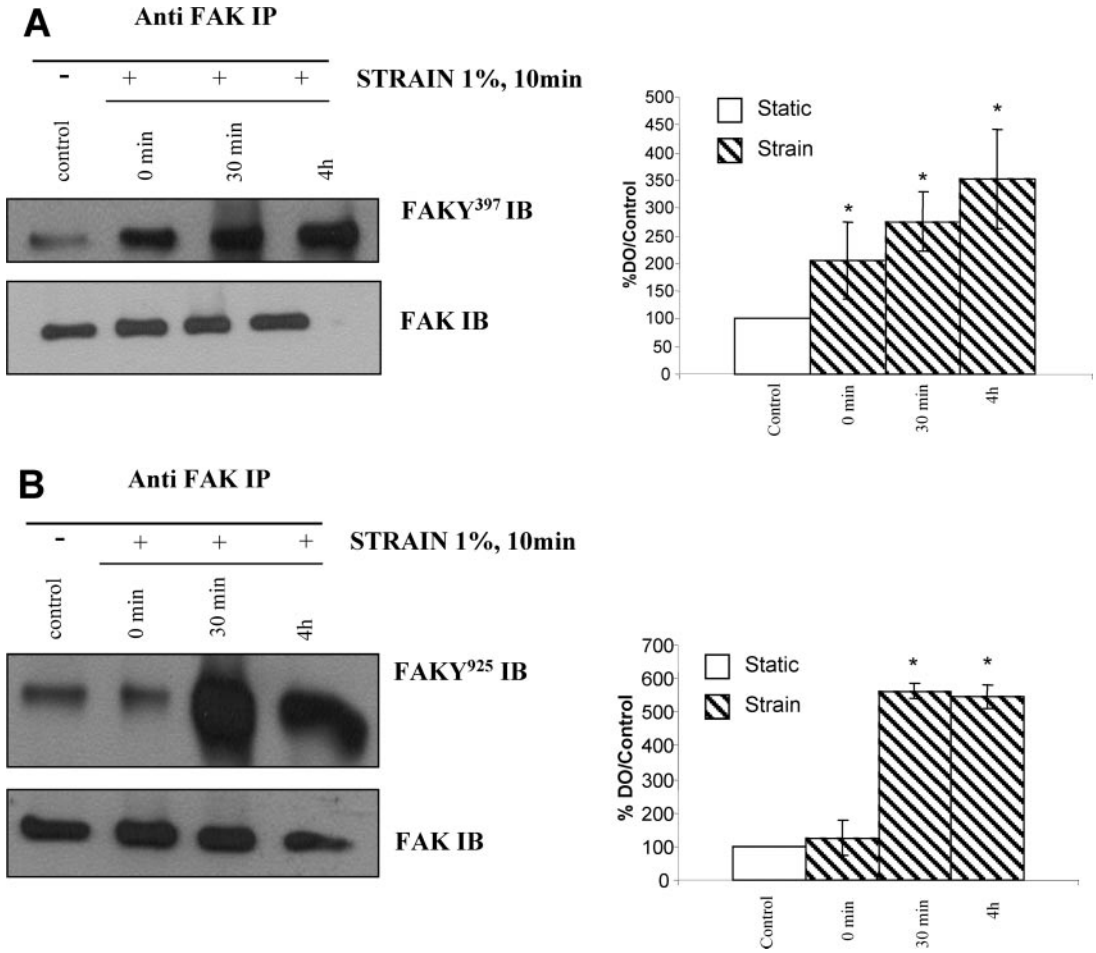

FIG. 4. **FAK phosphorylation at Tyr-397 (*A*) and Tyr-925 (*B*) in response to cyclic strain.** ROS 17/2.8 cells plated on flexible bottomed culture plates were subjected to strain for 0 (*C*) or 10 min. Cells were lysed immediately (*0 min*), 30 min, or 4 h after the end of strain. Lysates were immunoprecipitated with an anti-FAK rabbit polyclonal antibody (C-20) (*Anti FAK IP*). Immunoprecipitates were analyzed by SDS-PAGE followed by transfer of proteins and immunoblotting with an anti-FAK-Tyr(P)-397 (*FAKY^{397} IB*) (*A*) or an anti-FAK-Tyr(P)-925 (*FAKY^{925} IB*) (*B*) rabbit phosphospecific antibody. The blot was then stripped and reblotted with an anti-FAK mouse monoclonal antibody (H-1) (*FAK IB*). Quantification of FAK phosphorylation was performed by densitometric scanning of the bands. Values shown are the mean ± S.E. of at least three experiments. (*, $p < 0.05$).

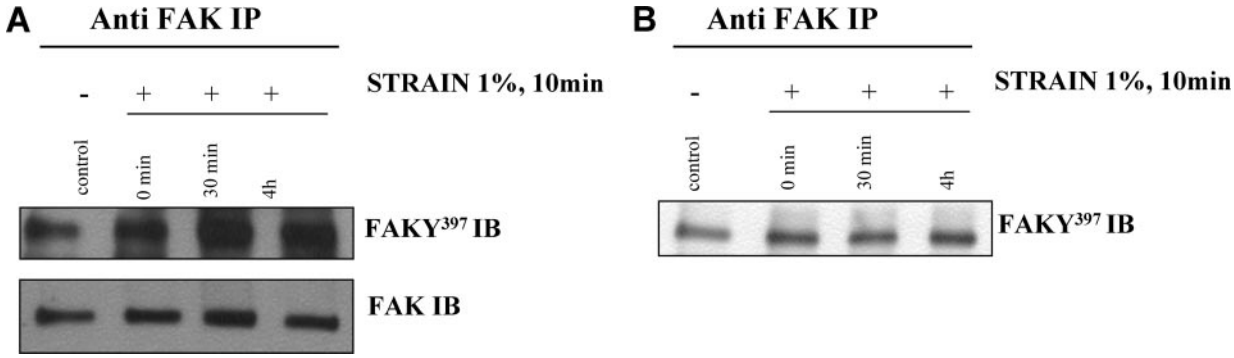

FIG. 5. **FAK phosphorylation at Tyr-397 in response to cyclic strain on osteoblastic MC3T3 cells (*A*) and osteoblastic cells obtained from rat metaphysis enzymatic digestion (*B*).** Cells plated on flexible bottomed culture plates were subjected to strain for 0 min (*control*) or 10 min. Cells were lysed immediately (*0 min*), 30 min, or 4 h after the end of strain. Lysates were immunoprecipitated with an anti-FAK rabbit polyclonal antibody (C-20) (*Anti FAK IP*). Immunoprecipitates were analyzed by SDS-PAGE followed by transfer of proteins and immunoblotting with an anti-FAK-Tyr(P)-397 (*FAKY^{397} IB*) rabbit phosphospecific antibody. The blot was then stripped and reblotted with an anti-FAK mouse monoclonal antibody (H-1) (*FAK IB*).

Transient Transfection in Rat ROS17/2.8 Cells—pcDNA3.1/lacZ control vector (pcDNA3 vector), pcDNA3-PYK2Y402F, and the pcDNA3-FAKY397F vector were transfected into ROS 17/2.8 cells with LipofectAMINE™ 2000 according to the manufacturer's recommendation (Invitrogen). After 24 h, cells were fed fresh medium and allowed to grow for 1 day. Cells were then placed in serum-free medium overnight and then submitted to static or strained conditions as described above in the paragraph entitled "Cyclic Deformation." Cells were then lysed in lysis buffer. Lysates were analyzed by immunoprecipitation followed by immunoblotting with specific antibodies. On average, 30% of the cells were highly stained as determined by 5-bromo-4-chloro-3-indolyl β-D-galactopyranoside (X-gal) staining. We also obtained similar results when we transfected ROS 17/2.8 with HA-FAKY397F and then immunostained with the HA antibody (not shown).

Statistics—All data were obtained from at least two independent experiments performed in triplicate. Results were expressed as mean ±

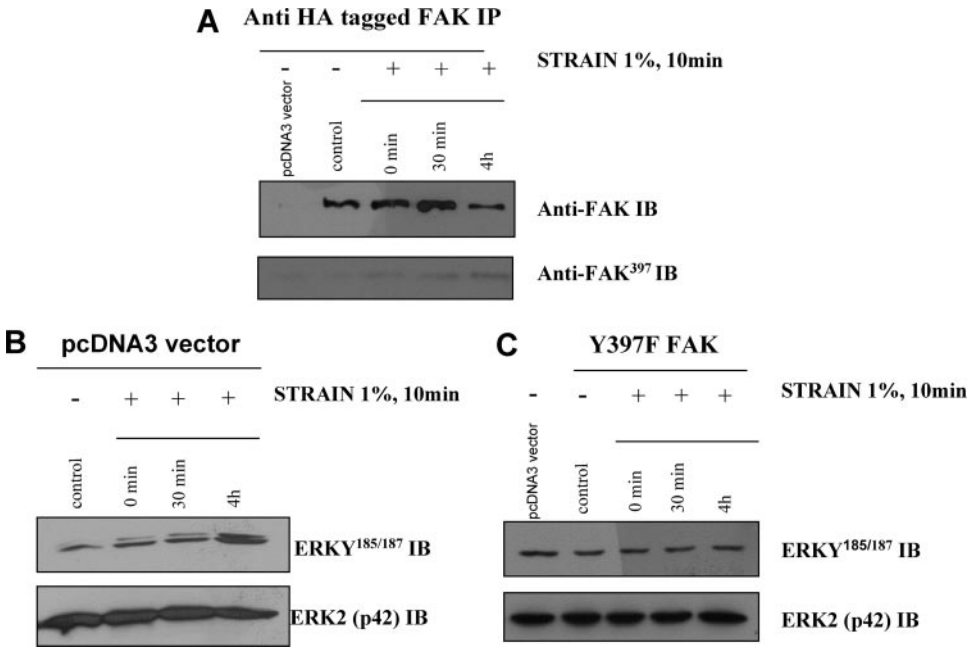

FIG. 6. **Cell transfection with FAK mutated at Tyr-97 suppressed the strain-induced phosphorylation of ERK2 at Tyr-187.** ROS 17/2.8 cells were transfected with the mutant FAK-Y397F or pcDNA3.1/lacZ control vector (pcDNA3 vector). Lysates were immunoprecipitated with an anti-HA mouse monoclonal antibody. Immunoprecipitates (*IP*) were analyzed by SDS-PAGE followed by the transfer of proteins and immunoblotting with an anti-FAK-Tyr(P)-397 rabbit phosphospecific antibody (*Anti-FAK^{397} IB*) (*A*), or the lysates were immunoblotted with a rabbit polyclonal anti-ERK1/2 MAPK Tyr(P)-185/187 phosphospecific antibody (*ERKY$^{185/187}$ IB*) (*B* and *C*). Equal protein loading was routinely verified by stripping the blot and reblotting with an anti-ERK2 mouse monoclonal antibody (*ERK (p42) IB*).

S.E. Statistical analyses were performed with Mann-Whitney's non-parametric test for unpaired samples. A p value of <0.05 was considered significant.

RESULTS

Strain-induced Proliferation—In this experiment, ROS 17/2.8 cell proliferation was analyzed 24 and 48 h after strain stimulation. As shown in Fig. 1*A*, the fraction of cells in each generation can be assessed by the PI, a measure of the proliferation activity of total cell population. ROS 17/2.8 cells submitted to cyclic strain were more numerous than unstrained cells at 24 h as well as at 48 h after a 10-min strain period (Fig 1*A*). Indeed, in a typical 48-h experiment as shown by both the FL2 histogram (*i.e.* PKH-26 profile; Fig 1*B*, *upper panel*) and the percentages of cells in each generation (Fig 1*B*, *table*), the strained cell numbers were 24.9 ± 1.4% and 52.4 ± 2.4% in the second and the third generation, respectively, whereas the unstrained cell numbers were 66.14 ± 1.9% and 9.3 ± 3.2% in the second and the third generation, respectively.

MEK Inhibition Blocked Strain-induced Proliferation—We hypothesized that the mitogenic cyclic strain was mediated by MEK pathway activation. Treatment of the culture medium with the MEK inhibitor PD-98059 (20 μM) during the 24- or 48-h incubation period did not affect the cell morphology, at least not at the light microscopic level, but completely blocked strain-induced proliferation. PD-98059-treated static monolayers in the same experiment proliferated equivalently to static monolayers in control or Me_2SO-treated media, but no increase in proliferation was observed in response to strain (Fig 1*A*). No effect on either basal or strain-stimulated proliferation was observed with the Me_2SO vehicle control.

Cyclic Strain Phosphorylated ERK—Because cyclic strain stimulated ROS 17/2.8 proliferation, we measured ERK phosphorylation in time course experiments using phosphospecific antibodies. Cyclic strain induced ERK2 phosphorylation in a time-dependent manner in contrast to the case with ERK1, which was weakly phosphorylated. Strain-induced ERK2 at Tyr-187 phosphorylation increased progressively from 0 min to 4 h after strain up to 429 ± 84% of control ($p < 0.05$; $n = 3$) as measured by densitometric scanning (Fig. 2).

Identification of Phosphotyrosine-containing Proteins Induced by Cyclic Strain—To investigate the involvement of upstream protein tyrosine phosphorylation involved in stretch-induced ERK activation, tyrosine phosphorylation of cellular proteins was examined by immunoblotting using an anti-phosphotyrosine monoclonal antibody. In response to cyclic strain, a time-dependent tyrosine phosphorylation of several proteins was observed in ROS 17/2.8 cells (Fig. 3) as well as in the mouse osteoblastic cell line MC3T3-E1 (data not shown). These proteins included broad bands of 125, 116, 68, and 60 kDa. The increase in the tyrosine phosphorylation level was detected as early as the end of strain and was extended up to 4 h. Under basal conditions (*i.e.* after an overnight serum starvation), a significant level of protein tyrosine phosphorylation was observed, probably because of integrin-mediated protein tyrosine phosphorylation linked to the extracellular matrix adhesion (43). Because major tyrosine-phosphorylated proteins were detected at 60–70 and 110–125 kDa, we examined the involvement of the tyrosine phosphorylations of pp125^{FAK} (125 kDa) (44), Src (60 kDa) (45), and PYK2 (116 kDa) (46).

Tyrosine Phosphorylation of pp125^{FAK} Induced by Cyclic Strain—pp125^{FAK} was immunoprecipitated from lysates of static and stretched cells with the anti-FAK rabbit polyclonal antibody and probed with the anti-FAK-Tyr(P)-397 or the anti-FAK-Tyr(P)-925 rabbit phosphospecific antibodies. The level of tyrosine phosphorylation at FAK-Tyr-397 and FAK-Tyr-925 from stretched cells was higher as compared with that of static cells. These results were found in ROS17/2.8 cells (Fig. 4) as well as in MC3T3-E1 (Fig 5*A*) cells and primary rodent osteoblastic cells (Fig 5*B*). FAK-Tyr-397 phosphorylation increased in a time-dependent manner (Fig 4*A*). As for FAK-Tyr-925 phosphorylation, it began 30 min after strain (Fig 4*B*) and remained at the same level at 4 h after strain (*i.e.* 463 ± 23% of static controls). Interestingly, a ROS 17/2.8 cell transfection with FAK mutated at Tyr-397 (Fig 6*A*) suppressed the strain-

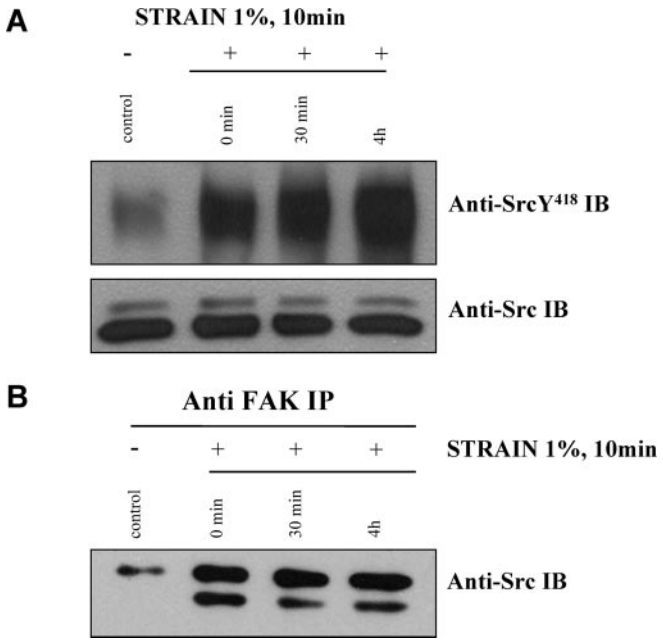

FIG. 7. **Src phosphorylation at Tyr-418 (Y^{418})and coimmunoprecipitation of FAK with Src in response to cyclic strain.** ROS 17/2.8 cells plated on flexible bottomed culture plates were subjected to strain for 0 min (*control*) or for 10 min. Cells were lysed immediately (*0 min*), 30 min, or 4 h after the end of strain. Lysates were analyzed by SDS-PAGE followed by the transfer of proteins and immunoblotting with an anti-rabbit phosphospecific antibody (*Anti-$SrcY^{418}$*. The blot was then stripped and reblotted with an anti-Src mouse monoclonal antibody B-12 (*Anti-Src IB*) (*A*). Lysates from ROS 17/2.8 were immunoprecipitated using anti-FAK rabbit polyclonal antibody C-20. The immune complexes were then Western blotted with an mouse monoclonal anti-Src antibody B-12 (*B*).

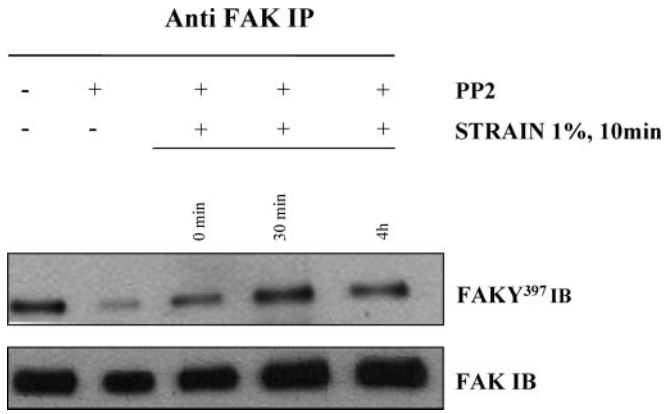

FIG. 8. **Role of Src family kinases activity in FAK phosphorylation at Tyr-397 in response to cyclic strain.** Cells plated on flexible bottomed culture plates were treated for 30 min in the absence (−) or presence (+) of PP2 (10 μM) before a 10-min stretch period. Cells were lysed immediately (*0 min*), 30 min, or 4 h after the end of strain. Lysates were immunoprecipitated with an anti-FAK rabbit polyclonal antibody (C-20) (*Anti FAK IP*). Immunoprecipitates were analyzed by SDS-PAGE followed by transfer of proteins and immunoblotting with an anti-FAK-Tyr(P)-397 rabbit phosphospecific antibody (*$FAKY^{397}$ IB*). The blot was then stripped and reblotted with an anti-FAK mouse monoclonal antibody (H-1) (*FAK IB*).

induced phosphorylation of ERK2 at Tyr-187 (Fig 6*C*), whereas transfection with an unrelated sequence (lacZ) did not prevent the ERK2 phosphorylation observed at the same time points in non-transfected cells (Fig 6*B*).

Tyrosine Phosphorylation of Src Family Tyrosine Kinase Induced by Cyclic Strain and the Role of Src Family Kinase Activity in FAK Phosphorylation in Response to Mechanical Strain—Src family kinases are important for generating adhesion-mediated tyrosine phosphorylation of FAK (28). Phosphorylation of Src proteins was analyzed from static and stretched cell lysates by SDS-PAGE followed by the transfer of proteins and immunoblotting with an anti-Src pY418 rabbit-phosphospecific antibody. Strain induced a dramatic increase in the level of tyrosine phosphorylation of Src at Tyr-418 as compared with static cells (Fig 7*A*). This increase occurred as early as the end of stretch and persisted up to 4 h after strain. Coimmunoprecipitation of Src with FAK showed that the interaction between these two proteins was increased by strain as early as the end of strain and up to 4 h (Fig 7*B*). To examine the role of Src family kinases in the strain-induced phosphorylation of FAK at Tyr-397, we analyzed the effect of pyrazolopyrimidine PP-2, a selective inhibitor of Src family kinase members (48), on FAK Tyr-397 phosphorylation induced by mechanical strain. ROS17/2.8 cells were treated with PP-2 (10 μM) 30 min before strain, a procedure that was shown previously to inhibit Src family activation (49). Cell lysates were immunoprecipitated with an anti-FAK antibody, and the immune complexes were analyzed by SDS-PAGE followed by Western blotting with a phosphospecific antibody directed against the autophosphorylation of FAK (anti-FAK-Tyr(P)-397 antibody). Treatment with PP-2 markedly reduced the phosphorylation at Tyr-397 in basal conditions. PP2 did not prevent the FAK phosphorylation at Tyr-397 induced by mechanical strain, suggesting a Src-independent early activation of FAK. In contrast, PP2 treatment strongly reduced the strain-induced increase in FAKY397 activation observed at 4 h. (Fig. 8).

Mechanical Strain Induced an Increase in Focal Adhesion Plaque Number and Size—It is well established in other cell types such as endothelial or smooth muscle cells that integrins are mechanotransducers. Because mechanical strain-induced integrin involvement is known to activate FAK in endothelial or smooth muscle cells (50, 51), we hypothesized that the tyrosine phosphorylation events we observed occurred at focal contacts, *i.e.* the signal transduction functional units of integrins. Subconfluent cells were exposed to a 10-min strain, fixed, and examined by indirect immunostaining for phosphotyrosine residues using a Tyr(P) (PY99) antibody (Fig 9*A*) and for tyrosine phosphorylation of FAK at Tyr-397 using a polyclonal FAK-Tyr-397 (data not show). Unstrained cells were similarly stained. In fact, Tyr(P) and FAK-Tyr-397 cell staining localized essentially to focal adhesion plaques. Staining was more intense in strained cells as compared with control cells. This was confirmed by measuring the mean phosphotyrosine spot number per cell, which was 166% of static control immediately after strain, and the mean phosphotyrosine spot area, which exhibited a 241% increase at 2 h (Fig 9*B*).

Tyrosine Phosphorylation of PYK2 Induced by Cyclic Strain and Ca^{2+} Involvement—PYK2 has been shown to display an integrin-dependent phosphorylation in lymphocyte B, CMK cells, and transfected COS cells (52, 53) and was recently shown to be activated by mechanical strain in smooth muscle cells (54). The level of PYK2 tyrosine phosphorylation at Tyr-402 from stretched cells occurred at 30 min with a major peak at 4 h (292 ± 95% increase as compared with static controls) (Fig 10). Cell transfection with PYK2 mutated at Tyr-402 abolished ERK2 tyrosine phosphorylation in unstrained controls. Moreover, PYK2 mutation dramatically reduced phosphorylation of ERK2 at Tyr-187 induced by strain, even though a weaker PYK2 mechanical strain activation persisted 4 h after strain (Fig 11). Coimmunoprecipitation of PYK2 with FAK showed that the association between these two proteins increased with strain in a time-dependent manner (Fig 12). Interestingly, PYK2 coimmunoprecipitated with Src, but in contrast to the case with FAK, this association was not increased by strain (not shown).

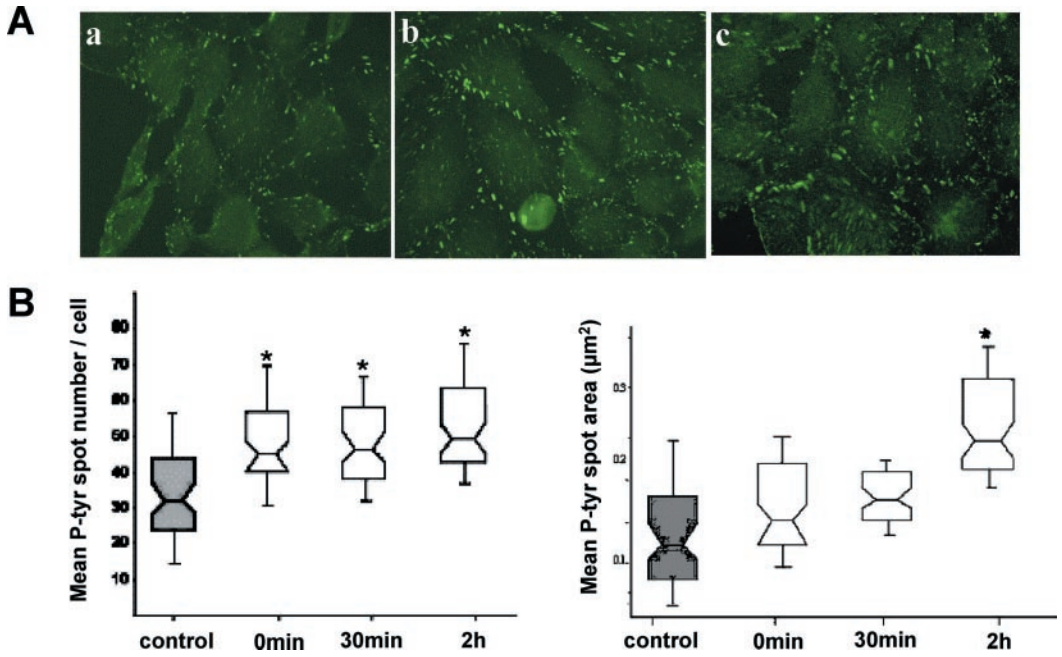

FIG. 9. **Microscopic views of Tyr(P) (*P-tyr*) immunostaining (PY99) in static and strained cells (*A*) and quantitative image analysis of phosphotyrosine positive spots (*B*).** *A*, confluent monolayers of ROS17/2.8 were kept as static controls (*a*) or subjected to a cyclic strain of 1% for 10 min. Cells were then fixed and immunostained immediately after strain (*b*) or 4 h after strain (*c*) with a monoclonal anti-phosphotyrosine (PY99). Primary antibody was detected by a fluorescein isothiocyanate-conjugated goat anti-rabbit antibody. *B*, results of image analysis and quantification phosphotyrosine spot staining. ROS 17/2.8 cells were strained during a single 10-min period. They were then fixed at different time points during the recovery period. *Left panel*, mean phosphotyrosine spot number per cell; *right panel*, mean phosphotyrosine spot area. *Gray boxes*, control untrained cells; *empty boxes*, strained cells. Values are median (25th to 75th percentiles). *, significant differences at $p < 0.05$ are *versus* controls.

It has been shown that the elevation of intracellular calcium concentrations is crucial for PYK2 activation (31) and is involved in mechanical signal transduction (55). To determine whether accumulation of Ca^{2+} contributes to the activation of PYK2, we examined the phosphorylation of PYK2 after pretreatment with the intracellular Ca^{2+} chelator BAPTA-AM. BAPTA-AM partially inhibited strain activation of PYK2 at Tyr-402, even though a weak increase was observed under mechanical strain (Fig 13) as compared with the kinetics observed without BAPTA-AM (Fig 10). Furthermore, treatment with thapsigargin, an agent that specifically inhibits the endoplasmic reticulum Ca^{2+}-ATPase, immediately increased PYK2 phosphorylation (Fig 13) and therefore fully prevented the strain-induced peak observed at 4 h after strain, although it did not influence the peak observed earlier at 30 min. After extracellular Ca^{2+} chelation by EGTA, strain-induced phosphorylation of PYK2 at Tyr-402 occurred unchanged at 30 min, although it was dramatically diminished 4 h after strain. These data suggested that PYK2 late activation was dependent on both intracellular Ca^{2+} release from ergastoplasmic stores and extracellular Ca^{2+} entry.

DISCUSSION

Mechanotranduction plays a key role in the biological processes of a variety of cell types, including smooth muscle cells (54), endothelial cells (56–58), and bone cells (59). It involves the conversion of a biophysical force into a cellular/molecular response leading to both rapid changes in kinase-mediated gene expression as well as slower adaptive changes in cytoskeletal arrangement. In the case of bone, a mechanical strain applied at appropriate levels *in vivo* was shown to increase bone mass through an increase in osteoblastic formation due to a likely stimulation of osteoblastic cell recruitment (60). Several studies showed that MAPKs have been linked to the regulation of proliferation in response to various stimuli in several cell types, including osteoblasts (5, 59, 61). Moreover, strain is known to activate ERK1/2 and P38 MAPK; however the patterns and time courses of activation of each MAPK appear to vary with cell types and the force applied (63–65). In the present study, we found that a 10-min stretch period was able to increase ROS 17/2.8 cell proliferation significantly after 48 h in serum-free medium. These findings were reproduced in rat primary osteoblastic cells after a period of 8 days in the presence of serum (66). These experiments were carried out with cyclic strain at 1% deformation, which was above the upper limit of the physiological range as measured in the limb bones of athletes (67).

The effects of cyclic strain on ROS 17/2.8 proliferation were blocked by PD-98059, a MEK inhibitor that prevents ERK1 and ERK2 activation. Although PD-98059 could have other effects, the concentration used here is consistent with that previously used to inhibit ERK activation (41, 68). Moreover, this treatment did not alter the proliferation rate as compared with vehicle treated controls. The ERK pathway has long been reported as being activated by mechanical stimulus in osteoblasts. However, most of the studies used fluid flow (9–12) to produce shear stress on bone cells. It is not well established whether the bone cell response to mechanical stimulus is unequivocal. Indeed, Smalt *et al.* (18) showed that bone cells increased nitric oxide and prostaglandin E2 production under shear stresses, although the cells did not respond to stretch in their models. Interestingly, Jessop *et al.* found that ERK activation patterns differed between both stimuli (15). In addition, centrifugation, which has also been used as a mechanical stimulus *in vitro*, did induce ERK activation in MC3T3 cells; however, FAK phosphorylation did not occur in this model (13), whereas it was observed in our work. Altogether, these data demonstrate that, whereas various stimuli appear to be relevant in terms of bone physiology, they are not redundant in terms of molecular events Moreover, the type and stage of differentiation also modulate mechanically induced ERK acti-

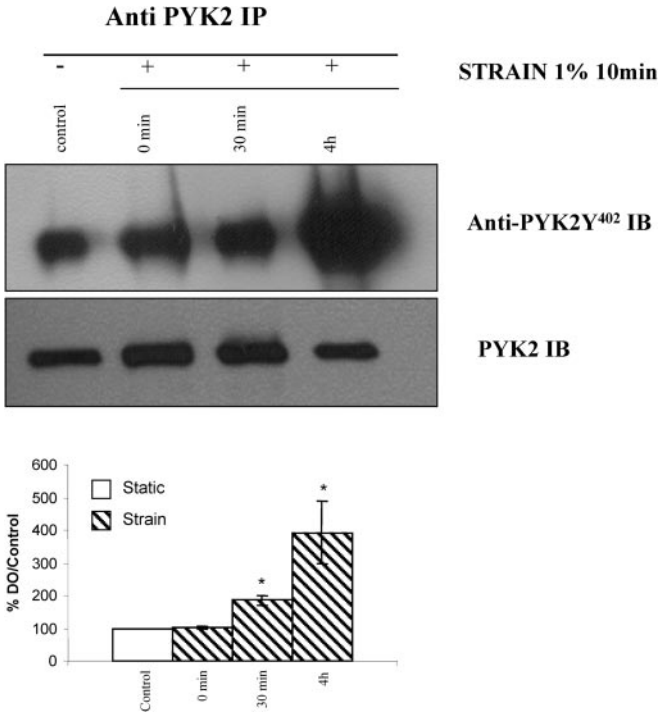

FIG. 10. **PYK2 phosphorylation at Tyr-402 in response to cyclic strain.** ROS 17/2.8 cells plated on flexible bottomed culture plates were subjected to strain for 0 min (*control*) or for 10 min. Cells were lysed immediately (*0 min*), 30 min, or 4 h after the end of strain. Lysates were immunoprecipitated with an anti-PYK2 mouse monoclonal antibody. Immunoprecipitates were analyzed by SDS-PAGE followed by transfer of proteins and immunoblotting with an anti-PYK2-Tyr(P)-402 rabbit phosphospecific antibody (*Anti-PYK2Y^{402} IB*). Equal protein loading was routinely verified by immunoblotting with an anti-PYK2 mouse monoclonal antibody (*PYK2 IB*). Quantification of PYK2-Tyr(P)-402 was performed by densitometric scanning of the bands. Values were expressed as mean ± S.E. (*$p < 0.05$; $n = 3$).

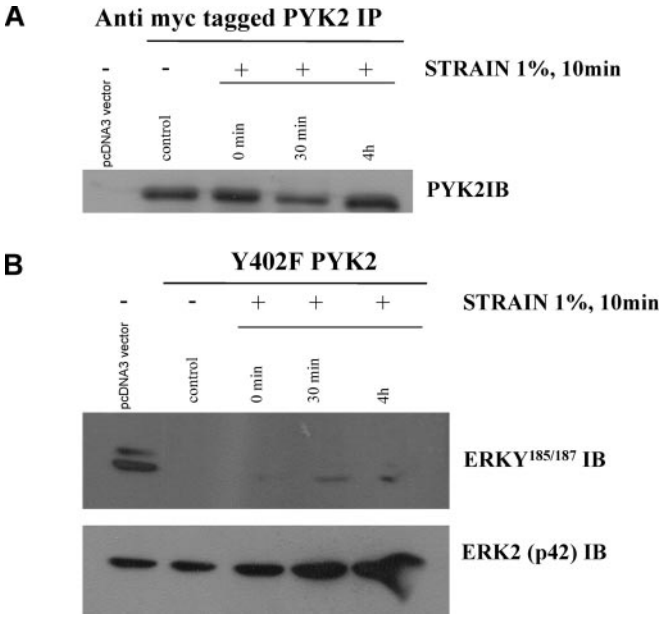

FIG. 11. **Cell transfection with PYK2 mutated at Tyr-402 modifies the strain-induced phosphorylation of ERK2 at Tyr-187.** ROS 17/2.8 cells were transfected with mutants PYK2-Y402F or pcDNA3.1/lacZ control vector (pcDNA3 vector). Lysates were immunoprecipitated (*IP*) with an anti-Myc mouse monoclonal antibody. Immunoprecipitates were analyzed by SDS-PAGE followed by transfer of proteins and immunoblotting with an anti-PYK2 mouse monoclonal antibody (*PYK2IB*) (*A*), or lysates were immunoblotted with the rabbit polyclonal anti-ERK1/2 MAPK Tyr(P)-185/187 phosphospecific antibody (*ERKY$^{185/187}$ IB*) (*B*). Equal protein loading was routinely verified by stripping the blot and reblotting with an anti-ERK2 mouse monoclonal antibody (*ERK2 (p42) IB*).

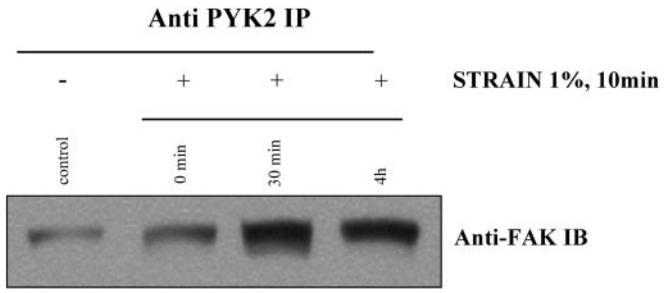

FIG. 12. **Strain-induced coimmunoprecipitation of FAK with PYK2 in a time-dependent manner.** Lysates from ROS 17/2.8 cells were immunoprecipitated using anti-PYK2 mouse monoclonal antibody (*Anti PYK2 IP*). The immune complexes were then Western-blotted with monoclonal anti-FAK antibody (H-1) (*Anti-FAK IB*).

vation. Matsuda *et al.* (69) reported no change in ERK phosphorylation after stretch in PDL cells; however, in this latter study the strain amplitude was much higher (9%) than that used in our study. Adhesive interactions with extracellular matrix components play a critical role in regulating intracellular signaling pathways that control cell growth, survival, and differentiation. On the one hand, the integrin family of transmembrane cell surface receptors mediates cell contact with the extracellular matrix, which is responsible for initiating the formation of focal adhesion structures, including the recruitment of FAK. This event is followed by the subsequent activation of the ERK pathway. On the other hand, focal adhesions have been proposed as a site for the cellular perception of external mechanical forces in a variety of cell types (70). Indeed, mechanical stretch activates the ERK pathway through interaction with FAK in intestinal epithelial cells (20). However, the relationships between integrin and ERK activation induced by mechanical strain in osteoblasts are not fully understood. In this report, we showed for the first time that mechanical strain rapidly activated FAK-Tyr-397 phosphorylation followed by FAK-Tyr-925 phosphorylation in osteoblasts. Furthermore, we observed a similar FAK-Tyr-397 phosphorylation in rat primary osteoblasts and MC3T3 osteoblastic cells, demonstrating that ROS17/2.8 cells are a valid model. These data are in line with previous reports that showed a mechanical strain-induced FAK-Tyr-397 phosphorylation *in vitro* and *in vivo* (72, 73) in fibroblasts and in the heart, respectively. Upon integrin binding, FAK autophosphorylation at tyrosine residue 397 is followed by phosphorylation by other tyrosine kinases at other sites, including FAK-Tyr-925. FAK-Tyr-925 Grb2 binding leads to the activation of the Ras/MAPK signal transduction pathway (30). It has been shown that integrin-dependent ERK activation can occur independently of FAK through Shc phosphorylation (74). However, in our study, transfection with FAK mutated at Tyr-397 abolished phosphorylation of ERK2 at Tyr-187, demonstrating that strain-induced FAK-Tyr-397 phosphorylation is definitely required for strain activation of ERK.

The phosphorylation of FAK at Tyr-397 triggers the formation of molecular complexes with other signaling proteins, including Src family kinases (25), the p85 regulatory subunit phosphatidylinositol 3-kinase (75), the phospholipase Cγ-1 (76), the adapter proteins Grb-7 (77) and Shc (78), and the tumor suppressor PTEN (79). The best characterized function of FAK at Tyr-397 is the creation of a high affinity binding site for the Src homology 2 domain of Src family members (29). In this study, mechanical stimulation induced an increase in FAK-Src coimmunoprecipitate levels far above the control lev-

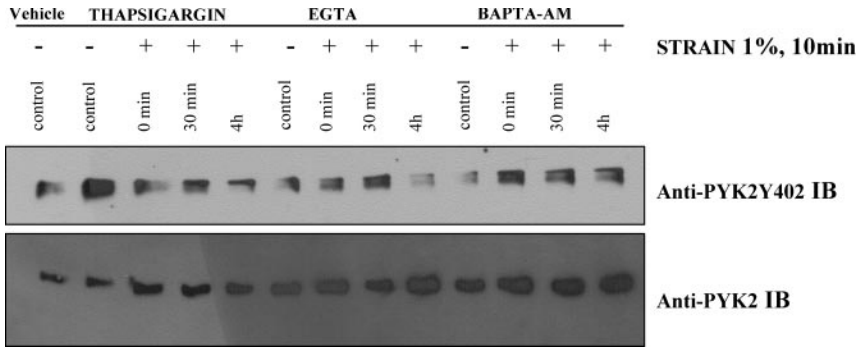

FIG. 13. **Calcium involvement in strain-induced PYK2 activation.** Serum-starved ROS17/2.8 cells were pretreated with thapsigargin (2 μM), EGTA (3 mM), BAPTA-AM (10 μM), or vehicle (dimethyl sulfoxide) for 15 min followed by mechanical strain for 10 min. Cells were lysed immediately (*0 min*), 30 min, or 4 h after the end of strain. Lysates were immunoblotted with an anti-PYK2-Tyr-402 rabbit phosphospecific antibody (*Anti-PYK2pY402 IB*). Equal protein loading was routinely verified by stripping the blot and reblotting with an anti-ERK2 mouse monoclonal antibody (*Anti-PYK2 IB*).

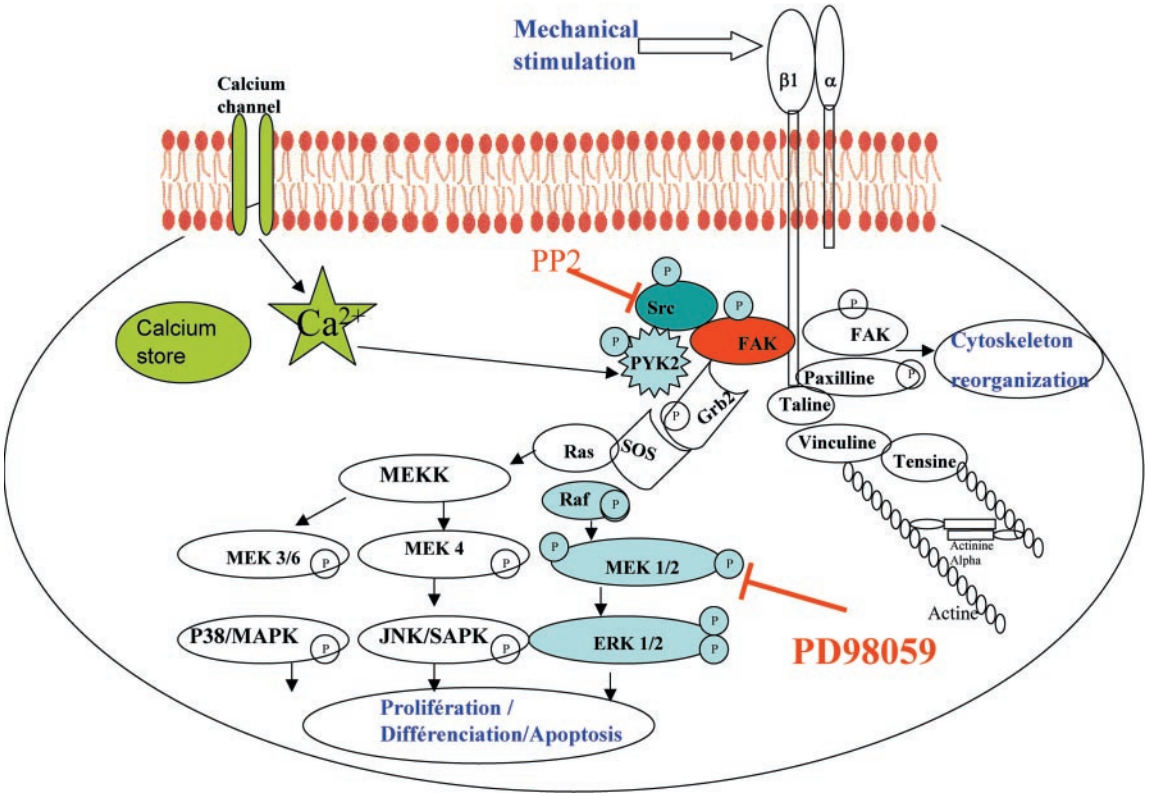

FIG. 14. **Model for mechanism of signaling events via FAK and PYK2 phosphorylation in response to mitogenic cyclic strain.** *MEK*, MAPK/ERK kinase; *MEKK*, MEK kinase; *JNK*, c-Jun N-terminal kinase; *SAPK*, stress-activated protein kinase.

els as early as the end of strain that persisted up to 4 h. Interestingly, we found that pretreatment with PP-2, a selective inhibitor of Src family kinases, markedly reduced the phosphorylation at Tyr-397 in basal conditions as reported previously (49). Interestingly, PP2 did not prevent mechanical strain-induced FAK-Tyr-397 activation at 30 min but strongly reduced the activation observed at 4 h. Thus, our data suggest that the high levels of FAKY397 phosphorylation observed 4 h after mechanical strain are consistent with the observation that FAK-Src association can lead to the recruitment of other signaling molecules to the complex with the subsequent strengthening of FAK-Tyr-397 phosphorylation followed by transphosphorylation at additional sites such as Tyr-925 (28).

It is well evidenced that FAK phosphorylation occurs upon integrin binding to extracellular matrix motifs during cell adhesion (23, 24). However, the evolution of the FAK phosphorylation state in adherent cells that are submitted to mechanical strain remains poorly investigated. Pommerenke *et al.* showed that twisting magnetic beads coated with anti-β1 antibodies and bound to osteoblastic cells leads to FAK activation (14). In the present study, immunostaining of phosphotyrosine residues essentially localized to focal adhesion plaques. Staining was more intense in strained compared with control cells for Tyr(P) as well as for FAKY397 immunostaining. This finding was confirmed by measurements of mean phosphotyrosine spot number and area per cell. Interestingly, Tyr(P) spot number increase occurred as early as the end of strain, suggesting that strain rapidly induced formation of new focal contacts. In contrast, the spot area was significantly increased only at 4 h, suggesting that integrin clustering, illustrated by the growth of the focal contact size, was a later event in osteoblast cell adhesion adaptation to a new mechanical environment (80).

In addition to the pp125 band observed on the Tyr(P) Western blot of strained cell lysates, we found a 116-kDa migrating tyrosine-phosphorylated protein that we identified as PYK2. PYK2, a protein highly homologous to FAK, has only recently been reported as involved in cell response to mechanical stretch in smooth muscle cells (54). Interestingly, Freitas *et al.* (81) reported that fluoroaluminate, which is able to stimulate osteoblastic cell proliferation, induced both FAK and PYK2 activation, suggesting that these tyrosine kinases play a role in the anabolic effects of fluoride in bone. Thus, the anabolic effects of

mechanical strain on bone might be related to similar events. However, Jeschke *et al.* reported that fluoroaluminate induced a preferential PYK2 Src association (34), whereas in our study Src/FAK association increased after strain, and no such increase was observed between Src and PYK2 (not shown). In our study, the kinetics of PYK2 and FAK tyrosine phosphorylation differed with a late peak for PYK2 at 4 h, suggesting that the activation of these close tyrosine kinases might not be mediated by the same pathways. Moreover, PYK2 appeared to be required for strain activation of ERK; however, in contrast to the case with FAK, cell transfection with PYK2 mutated at Tyr-402 altered the basal phosphorylation of ERK2 at Tyr-187. The ERK2 mechanical strain-induced phosphorylation persisted, although weaker, at 30 min. In contrast, the peak observed at 4 h was completely abolished, demonstrating the critical role of PYK2 in late ERK activation. Thus, FAK and PYK2 both orchestrate ERK phosphorylation stimulated by mechanical strain. Interestingly, it has been shown that PYK2 directly phosphorylates FAK, raising the possibility that new docking sites for Src homology 2-containing proteins are generated on FAK (82). In return, FAK might modulate PYK2 activation by promoting a kinase substrate interaction. Indeed, we found that mechanical strain enhanced the association of FAK with PYK2 in a time-dependent manner.

It was shown that, during cell adhesion, clustering of integrins leads to the recruitment of FAK and PYK2 to the newly formed focal adhesion sites and activates the phosphorylation of a variety of downstream pathways (71). As for PYK2 activation mechanisms, it has been shown that this tyrosine kinase displays an integrin-dependent phosphorylation in lymphocyte B, CMK cells, and osteoclasts (52, 53, 62). However, a rapid rise in intracellular calcium concentration was reported to be the main activator of PYK2 (55). In addition, intracellular calcium transients are known to be the earliest responses detected in mechanically stimulated bone cells (31). In the present study, we showed that both pretreatment with EGTA or thapsigargin abolished strain-induced PYK2 activation 4 h after strain, suggesting that PYK2 phosphorylation at this time depended upon both calcium entry and release from endoplasmic reticulum stores. BAPTA-AM, a cell permeable calcium chelator, partially inhibited strain-induced PYK2 activation at Tyr-402 in a weaker manner than that observed with EGTA. Interestingly, in smooth muscle cells the late PYK2 activation induced by mechanical stretch was prevented by gadolinium chloride treatment, a stretch-activated cation channel inhibitor (54). In contrast, You *et al.* (9) found that the osteopontin mRNA increase observed in MC3T3-E1 osteoblastic cells under oscillatory fluid flow was completely abolished after the administration of an L-type voltage-operated calcium channel inhibitor, whereas gadolinium chloride had no effect. In fact, the role of stretch-activated channels in response to stretch remains controversial in osteoblasts (47). Altogether, our findings suggest that, although calcium has a regulatory role in PYK2 late activation, it is likely that other stimulating routes involved in PYK2 early activation do not depend on calcium.

In conclusion, we found that mitogenic mechanical strain increased the levels of tyrosine phosphorylation at focal contacts through an increase in both the number and size of adhesion plaques in osteoblasts-like cells. Mechanical strain promoted the association of the two highly homologous tyrosine kinases FAK and PYK2 and activated, with different kinetics, their tyrosine autophosphorylation sites, which were both critical for the full activation of ERK2. Src family kinases modulated FAK activation, whereas intracellular calcium levels were partly responsible for late PYK2 activation. As summarized in Fig. 14, these data suggest that both PYK2 and FAK orchestrate the early events promoting cell cycle progression induced by mechanical strain. Deciphering the other mechanisms potentially involved in FAK and PYK2 activation would lead to better understanding of beneficial effects of mechanical strain on bone.

Acknowledgment—We thank the Centre Commun de Cytométrie de Flux de Saint-Etienne.

REFERENCES

1. Oxlund, H., Andersen, N. B., Ortoft, G., Orskov, H., and Andreassen, T. T. (1998) *Endocrinology* **139,** 1899–1904
2. Banes, A. J., Tsuzaki, M., Yamamoto, J., Fischer, T., Brigman, B., Brown, T., and Miller, L. (1995) *Cell Biol.* **73,** 349–365
3. Wozniak, M., Fausto, A., Carron, C. P., Meyer, D. M., and Hruska, K. A. (2000) *J. Bone Miner. Res.* **15,** 1731–1745
4. Damien, E., Price, J. S., and Lanyon, L. E. (2000) *J. Bone Miner. Res.* **15,** 2169–2177
5. Lai, C. F., Chaudhary, L., Fausto, A., Halstead, L. R., Ory, D. S., Avioli, L. V., and Cheng, S. L. (2001) *J. Biol. Chem.* **276,** 14443–14450
6. Ingram, A. J., James, L., Cai, L., Thai, K., Ly, H., and Scholey, J. W. (2000) *J. Biol. Chem.* **275,** 40301–40306
7. Numaguchi, K., Eguchi, S., Yamakawa, T., Motley, E. D., and Inagami, T. (1999) *Circ. Res.* **85,** 5–11
8. Fanning, P. J., Emkey, G., Smith, R. J., Grodzinsky, A. J., Szasz, N., and Trippel, S. B. (2003) *J. Biol. Chem.* **278,** 50940–50948
9. You, J., Reilly, G. C., Zhen, X., Yellowley, C. E., Chen, Q., Donahue, H. J., and Jacobs, C. R. (2001) *J. Biol. Chem.* **276,** 13365–13371
10. Ogata T. (2000) *J. Cell. Biochem.* **76,** 529–538
11. Kapur, S., Baylink, D. J., and Lau, K. H. (2003) *Bone* **32,** 241–251
12. Weyts, F. A., Li, Y. S., van Leeuwen, J., Weinans, H., and Chien S. (2002) *J. Cell. Biochem.* **87,** 85–92
13. Hatton, J. P., Pooran, M., Li, C. F., Luzzio, C., and Hughes-Fulford, M. A. (2003) *J. Bone Miner. Res.* **18,**58–66
14. Pommerenke, H., Schmidt, C., Durr, F., Nebe, B., Luthen, F., Muller, P., and Rychly, J. (2002) *J. Bone Miner. Res.* **17,** 603–611
15. Jessop, H. L., Rawlinson, S. C., Pitsillides, A. A., and Lanyon, L. E. (2002) *Bone* **31,** 186–194
16. Basso, N., and Heersche, J. N. (2002) *Bone* **30,** 347–351
17. Miyauchi, A., Notoya, K., Mikuni-Takagaki, Y., Takagi, Y., Goto, M., Miki, Y., Takano-Yamamoto, T., Jinnai, K., Takahashi, K., Kumegawa, M., Chihara, K., and Fujita, T. (2000) *J. Biol. Chem.* **275,** 3335–3342
18. Smalt, R., Mitchell, F. T., Howard, R. L., and Chambers, T. J. (1997) *Am. J. Physiol.* **273,** E751–E758
19. Schmidt, C., Pommerenke, H., Durr, F., Nebe, B., and Rychly, J. (1998) *J. Biol. Chem.* **273,** 5081–5085
20. Zhang, J., Li, W., Sanders, M. A., Sumpio, B. E., Panja, A., and Basson, M. D. (2003) *FASEB J.* **17,** 926–928
21. Clark, E. A., and Brugge, J. S. (1995) *Science* **268,** 233–239
22. Alahari, S. K., Reddig, P. J., and Juliano, R. L. (2002) *Int. Rev. Cytol.* **220,** 145–184
23. Owen, J. D., Ruest, P. J., Fry, D. W., and Hanks, S. K. (1999) *Mol. Cell. Biol.* **19,** 4806–4818
24. Calalb, M. B., Polte, T. R., and Hanks, S. K. (1995) *Mol. Cell. Biol.* **15,** 954–963
25. Cobb, B. S., Schaller, M. D., Leu, T. H., and Parsons, J. T. (1994) *Mol. Cell. Biol.* **14,** 147–155
26. Xing, Z., Chen, H. C., Nowlen, J. K., Taylor, S. J., Shalloway, D., and Guan, J. L. (1994) *Mol. Biol. Cell* **5,** 413–421
27. Sieg, D. J., Hauck, C. R., Ilic, D., Klingbeil, C. K., Schaefer, E., Damsky, C. H., and Schlaepfer, D. D. (2000) *Nat. Cell Biol.* **2,** 249–256
28. Schlaepfer, D. D., Hauck, C. R., and Sieg, D. J. (1999) *Prog. Biophys. Mol. Biol.* **71,** 435–478
29. Schaller, M. D., Hildebrand, J. D., Shannon, J. D., Fox, J. W., Vines, R. R., and Parsons, J. T. (1994) *Mol. Cell. Biol.* **14,** 1680–1688
30. Schlaepfer, D. D., Hanks, S. K., Hunter, T., and van der Geer, P. (1994) *Nature* **372,** 786–791
31. Lev, S., Moreno, H., Martinez, R., Canoll, P., Peles, E., Musacchio, J. M., Plowman, G. D., Rudy, B., and Schlessinger, J. (1995) *Nature* **376,** 737–745
32. Sasaki, H., Nagura, K., Ishino, M., Tobioka, H., Kotani, K., and Sasaki, T. (1995) *J. Biol. Chem.* **270,** 21206–21219
33. Yu, H., Li, X., Marchetto, G. S., Dy, R., Hunter, D., Calvo, B., Dawson, T. L., Wilm, M., Anderegg, R. J., Graves, L. M., and Earp, H. S. (1996) *J. Biol. Chem.* **271,** 29993–29998
34. Jeschke, M., Standke, G. J., and Scaronuscarona, M. (1998) *J. Biol. Chem.* **273,** 11354–11361
35. Kassem, M., Mosekilde, L., and Eriksen, E. F. (1993) *J. Bone Miner. Res.* **8,** 1453–1458
36. Majeska, R. J., Rodan, S. B., and Rodan, G. A. (1980) *Endocrinology* **107,** 1494–1503
37. Banes, A. J., Gilbert, J., Taylor, D., and Monbureau, O. (1985) *J. Cell Sci.* **75,** 35–42
38. Yamamura, Y., Rodriguez, N., Schwartz, A., Eylar, E., Bagwell, B., and Yano, N. (1995) *Cell. Mol. Biol.* (*Noisy-Le-Grand*) **41,** Suppl. 1, S121–S132
39. Barani, A. E., Sabido, O., and Freyssenet, D. (2003) *Exp. Cell Res.* **283,** 196–205
40. Boutonnat, J., Muirhead, K. A., Barbier, M., Mousseau, M., Ronot, X., and Seigneurin, D. (1998) *Anticancer Res.* **18,** 4243–4251
41. Kumar, A., Middleton, A., Chambers, T. C., and Mehta, K. D. (1998) *J. Biol. Chem.* **273,** 15742–15748
42. Usson Y, Guignandon, A., Laroche, N., Lafage-Proust, M. H., and Vico, L. (1997) *Cytometry* **28,** 298–304

43. Burridge, K., Turner, C. E., and Romer, L. H. (1992) *J. Cell Biol.* **119,** 893–903
44. Schaller, M. D., Borgman, C. A., Cobb, B. S., Vines, R. R., Reynolds, A. B., and Parsons, J. T. (1992) *Proc. Natl. Acad. Sci. U. S. A.* **89,** 5192–5196
45. Cary, L. A., Chang, J. F., and Guan, J. L. (1996) *J. Cell Sci.* **109,** 1787–1794
46. Li, X., and Earp, H. S. (1997) *J. Biol. Chem.* **272,** 14341–14348
47. Peake, M. A., Cooling, L. M., Magnay, J. L., Thomas, P. B., and El Haj, A. J. (2000) *J. Appl. Physiol.* **89,** 2498–2507
48. Hanke, J. H., Gardner, J. P., Dow, R. L., Changelian, P. S., Brissette, W. H., Weringer, E. J., Pollok, B. A., and Connelly, P. A. (1996) *J. Biol. Chem.* **271,** 695–701
49. Salazar, E. P., and Rozengurt, E. (2001) *J. Biol. Chem.* **276,** 17788–17795
50. Ishida, T., Peterson, T. E., Kovach, N. L., and Berk, B. C. (1996) *Circ. Res.* **79,** 310–316
51. Seko, Y., Takahashi, N., Tobe, K., Kadowaki, T., and Yazaki, Y. (1999) *Biochem. Biophys. Res. Commun.* **259,** 8–14
52. Li, J., Avraham, H., Rogers, R. A., Raja, S., and Avraham, S. (1996) *Blood* **88,** 417–428
53. Astier, A., Avraham, H., Manie, S. N., Groopman, J., Canty, T., Avraham, S., and Freedman, A. S. (1997) *J. Biol. Chem.* **272,** 228–232
54. Iwasaki, H., Yoshimoto, T., Sugiyama, T., and Hirata, Y. (2003) *Endocrinology* **144,** 2304–2310
55. Hung, C. T., Pollack, S. R., Reilly, T. M., and Brighton, C. T. (1995) *Clin. Orthop.* **313,** 256–269
56. Takahashi, M., Ishida, T., Traub, O., Corson, M. A., and Berk, B. C. (1997) *J. Vasc. Res.* **34,** 212–219
57. Chen, K. D., Li, Y. S., Kim, M., Li, S., Yuan, S., Chien, S., and Shyy, J. Y. (1999) *J. Biol. Chem.* **274,** 18393–18400
58. Davies, P. F., and Tripathi, S. C. (1993) *Circ. Res.* **72,** 239–245
59. Dieudonne, M. N., Machinal-Quelin, F., Serazin-Leroy, V., Leneveu, M. C., Pecquery, R., and Giudicelli, Y. (2002) *Biochem. Biophys. Res. Commun.* **293,** 622–628
60. Bourrin, S., Palle, S., Genty, C., and Alexandre, C. (1995) *J. Bone Miner. Res.* **10,** 820–828
61. Valk, P., Verbakel, S., von Lindern, M., Lowenberg, B., and Delwel, R. (2000) *Hematol. J.* **1,** 254–263
62. Lakkakorpi, P.T., Bett, A. J., Lipfert, L., Rodan, G. A., and Duong, L. T. (2003) *J. Biol. Chem.* **278,** 11502–11512
63. Ingram, A. J., Ly, H., Thai, K., Kang, M. J., and Scholey, J. W. (1999) *Kidney Int.* **56,** 1721–1728
64. Ikeda, M., Takei, T., Mills, I., Kito, H, and Sumpio, B. E. (1999) *Am. J. Physiol.* **276,** 14–22
65. Matsuda, K., Yuasa, H., and Watanabe, J. (1998) *Biopharm. Drug Dispos.* **19,** 465–472
66. Guignandon, A., Akhouayri, O., Usson, Y., Rattner, A., Laroche, N., Lafage-Proust, M. H., Alexandre, C., and Vico, L. (2003) *Cell Commun. Adhes.* **10,** 69–83
67. Milgrom, C., Finestone, A., Simkin, A., Ekenman, I., Millgram, M., Nyska, M., Larsson, E., and Burr, D. (2000) *J. Bone Joint Surg.* **82,** 591–594
68. Ajizian, S. J., English, B. K., and Meals, E. A. (1999) *J. Infect. Dis.* **179,** 939–944
69. Matsuda, N., Morita, N., Matsuda, K., and Watanabe, M. (1998) *Biochem. Biophys. Res. Commun.* **249,** 350–354
70. Geiger, B., and Bershadsky, A. (2001) *Curr. Opin. Cell Biol.* **13,** 584–592
71. Avraham, H. K., Lee, T. H., Koh, Y., Kim, T. A., Jiang, S., Sussman, M., Samarel, A. M., and Avraham, S. (2003) *J. Biol. Chem.* **278,** 36661–36668
72. Wang, H. B., Dembo, M., Hanks, S. K., and Wang, Y. (2001) *Proc. Natl. Acad. Sci. U. S. A.* **98,** 11295–11300
73. Torsoni, A. S., Constancio, S. S., Nadruz, W., Jr., Hanks, S. K., and Franchini, K. G. (2003) *Circ. Res.* **93,** 140–147
74. Barberis, L., Wary, K. K., Fiucci, G., Liu, F., Hirsch, E., Brancaccio, M., Altruda, F., Tarone, G., and Giancotti, F. G. (2000) *J. Biol. Chem.* **275,** 36532–36540
75. Chen, H. C., Appeddu, P. A., Isoda, H., and Guan, J. L. (1996) *J. Biol. Chem.* **271,** 26329–26334
76. Zhang, X., Chattopadhyay, A., Ji, Q. S., Owen, J. D., Ruest, P. J., Carpenter, G., and Hanks, S. K. (1999) *Proc. Natl. Acad. Sci. U. S. A.* **96,** 9021–9026
77. Han, D. C., and Guan, J. L. (1999) *J. Biol. Chem.* **274,** 24425–24430
78. Schlaepfer, D. D., Jones, K. C., and Hunter, T. (1998) *Mol. Cell. Biol.* **18,** 2571–2585
79. Tamura, M., Gu, J., Danen, E. H., Takino, T., Miyamoto, S., and Yamada, K. M. (1999) *J. Biol. Chem.* **274,** 20693–20703
80. Kawakami, K., Tatsumi, H., and Sokabe, M. (2001) *J. Cell Sci.* **114,** 3125–3135
81. Freitas, F., Jeschke, M., Majstorovic, I., Mueller, D. R., Schindler, P., Voshol, H., Van Oostrum, J., and Susa, M. (2002) *Bone* **30,** 99–108
82. Li, X., Dy, R. C., Cance, W. G., Graves, L. M., and Earp, H. S. (1999) *J. Biol. Chem.* **274,** 8917–8924